Journal of Zhejiang University-SCIENCE B (Biomedicine & Biotechnology) *2022 23(9):778-783*
www.jzus.zju.edu.cn; www.springer.com/journal/11585
E-mail: jzus_b@zju.edu.cn

Correspondence

https://doi.org/10.1631/jzus.B2200233

Check for updates

Nanobubbles loaded with carbon quantum dots for ultrasonic fluorescence dual detection

Yankun ZHANG[2], Bingtao TANG[3], Yu XIN[1], Qiong WU[1], Lan LIU[1], Yunxia WANG[1], Kongxi ZHU[1], Guimei LIN[2], Hongjuan WANG[1]✉

[1]*Department of Gastroenterology, the Second Hospital of Shandong University, Jinan 250033, China*
[2]*School of Pharmaceutical Science, Shandong University, Jinan 250012, China*
[3]*School of Mechanical Engineering, Qilu University of Technology (Shandong Academy of Sciences), Jinan 250353, China*

To increase the efficiency and accuracy of clinical tumor detection, we explored multiple imaging by preparing carbon quantum dot (CQD)-loaded nanobubbles for ultrasonic fluorescence dual detection. In this experiment, we prepared 1,2-dioleoyl-3-trimethylammonium-propane chloride (DOTAP) cationic liposomes using the film dispersion method and chose perfluoropentane as the core gas material of the nanobubbles. The nanobubbles were coupled with the negatively charged CQDs through the charge effect to prepare the testing agent for two-way diagnosis with ultrasound contrast and fluorescence detection. The formulation and preparation of the loaded CQD liposome nanobubbles were screened. In vivo experiments showed that nanobubbles can be enriched to the tumor site within 5 min, which enables clearer ultrasound imaging and is conducive to tumor detection. We expect CQD-loaded liposome (Lip-CQD) nanobubbles to become a new ultrasonic contrast agent for clinical applications that can provide a basis for early tumor diagnosis and thus earlier treatment.

Cancer is a serious health and social issue. At present, the main clinical treatment approaches for tumors include surgery and systemic chemotherapy (Peng and Pei, 2021). However, the treatment effect is often poor for patients with advanced cancers, causing strong side effects and low quality of life. If the tumor can be detected and treated early, the prognosis can be significantly improved (Rathod et al., 2015). At present, tumor diagnoses can be divided into in vitro and in vivo diagnoses. In vitro diagnoses mainly involve taking blood samples from patients as a "liquid biopsy" or conducting a pathological examination of the tissue, primarily for histopathological examination and detection of tumor cells and tumor markers. Although the accuracy of these methods is high, their implementation is complicated, and the test results exhibit hysteresis.

Ultrasound imaging is a method of imaging tissues and organs in the body by receiving and processing reflected signals based on the principle that various organs and tissues reflect ultrasonic waves differently. This test is less or non-traumatic, convenient, and more affordable. It provides timely information for diagnosis and treatment by showing the current situation of the tumor through real-time imaging. In tissues with complex compositions, different densities, and even vacuoles, such as bone tissue, ultrasound can collect good signal echoes; however, in systems such as blood, which have low material density and low acoustic impedance, ultrasound relies on the strong reflection of ultrasound contrast agents to display clear echo images.

At present, most clinical agents are micron-sized contrast agents, also known as micron-sized bubbles, and their particle size distribution is in the range of 1–4 μm. The gas-liquid structure of the micron bubble can significantly enhance the contrast with the tissue background, thus improving the resolution of the echo reflection. The core-shell structure can alleviate damage and leakage in the body through the protective effect

✉ Hongjuan WANG, wanghongjuan2017@126.com
Hongjuan WANG, https://orcid.org/0000-0002-5019-8305

Received Apr. 24, 2022; Revision accepted Aug. 18, 2022;
Crosschecked Aug. 26, 2022

of the shell. Commonly used coating materials include albumin, surfactants, galactose, and lipid compounds. The materials usually selected for core gas are air, perfluoride, and nitrogen (Klibanov, 2005). In blood, micron bubbles injected intravenously are quickly cleared by the reticuloendothelial system and have a half-life of only a few minutes in serum (Willmann et al., 2008). Due to particle-size limitations, microbubbles have difficulty in penetrating tiny vasculature and are more difficult to concentrate in the tumor area, thereby limiting their imaging ability in small organs (Klibanov, 2005).

The structure of nanoscale contrast agents is similar to that of micron bubbles, and their shell materials are generally lipids, surfactants, or polymers, such as 1,2-dipalmitoyl-sn-glycero-3-phosphocholine (DPPC), poly(lactic-co-glycolic acid) (PLGA), or poly(lactic acid) (PLA). Under the action of ultrasonic waves, the nanobubbles expand and compress regularly, thus producing strong echo reflection, and the target site can be imaged via the sensor connected to the processor. Because of the small particle size, nanobubbles often have many special distribution behaviors, such as infiltration and enrichment of the tumor area (Fig. 1).

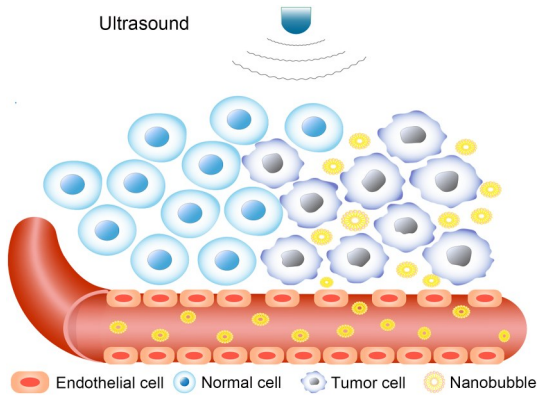

Fig. 1 Schematic illustration of nanobubble-based imaging. Process of using nanobubbles for imaging diseased tissues is as follows: after the nanovesicles are injected into the human body intravenously, they cannot pass through normal blood vessels but can freely enrich at the targeted sites through the diseased blood vessel space (380–780 nm); under the action of ultrasound, the nanobubbles burst or fuse, changing the echo characteristics of the site and thus enhancing imaging results.

The size of the nanoscale contrast agent, the selection of the core and shell materials, and the external active agents and ligands can all affect circulation time and absorption efficiency (Paefgen et al., 2015). Nanoscale contrast agents with smaller particle size have stronger penetration, weaker backscattering ability, and relative stability. By adjusting the composition, proportion, or preparation method of the film-forming material, the backscattering ability and the imaging effect can be further improved (Huang et al., 2001).

Fluorescence imaging is widely used, not only for real-time imaging but also for simultaneous multimolecular detection and multi-tissue imaging with high sensitivity. However, there are few fluorescence detection substances that can be clinically applied in the human body. In recent years, with the continuous exploration of biologically low-toxicity CQDs, it appears that CQDs are likely to become the next generation of clinical fluorescence detection agents. CQDs are a new type of fluorescent nanoscale carbon material. They are composed of spheroidal dispersed particles with a particle size of approximately 10 nm (Yang et al., 2019). CQDs are suitable for human fluorescence detection owing to their excellent biocompatibility (Zhu et al., 2015; Zhang et al., 2021) and low toxicity. The upsurge of research on CQDs stems from their good fluorescence properties, which include a stable fluorescence effect, high intensity, and an extensive excitation wavelength range. However, fluorescence detection agents are disturbed by fluorescent substances in the human body, which reduces the reliability of the detection results.

In general, exploring multiple and multidimensional imaging methods will make clinical testing more efficient and accurate. If two or more testing methods can be integrated to achieve the effects of a one-dose administration and multidimensional syndrome screening, detection efficiency and accuracy will be greatly improved, and this would provide a better means for accurately understanding the clinical course of patients and reducing the economic and mental burden of testing.

Our experiment revealed that when an ultrasonic cleaning instrument is used as the bubble-forming equipment, nanobubble particle size increases with higher ultrasonic power (Fig. 2a). However, there is no clear trend with ultrasonic time, because bubble size decreased, increased, decreased, and then increased (Fig. 2b). We investigated the influence of different crushing power and time parameters on the particle size of nanobubbles using an ultrasonic crushing apparatus. The results showed that the particle size of

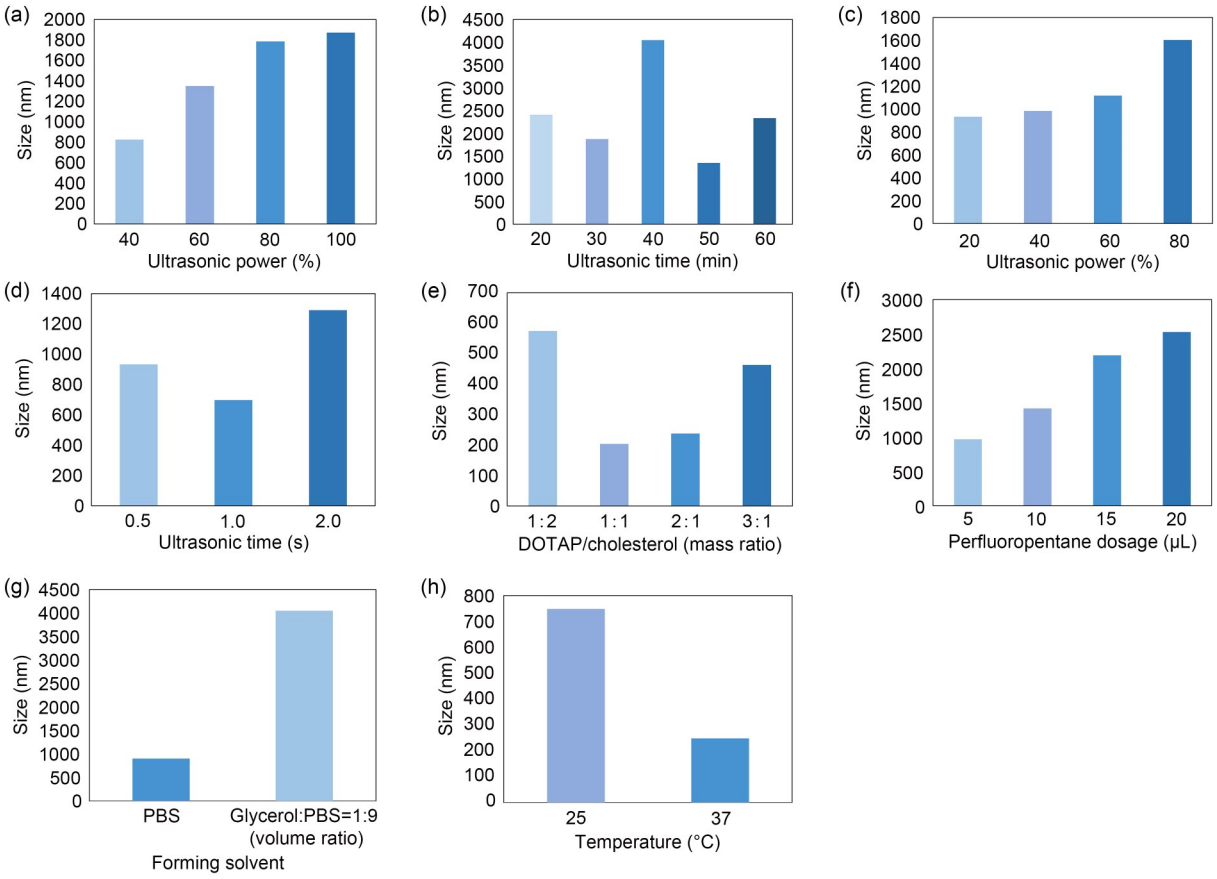

Fig. 2 Effects of preparation conditions on nanobubble size. (a) Power of ultrasonic cleaning instrument; (b) Time ultrasonic cleaning instrument; (c) Power of ultrasonic crushing instrument; (d) Time ultrasonic crushing instrument; (e) Mass ratio of DOTAP/cholesterol; (f) Perfluoropentane dosage; (g) Forming solvent; (h) Temperature. DOTAP: 1,2-dioleoyl-3-trimethylammonium-propane chloride; PBS: phosphate-buffered saline.

the liposome nanobubbles increased with increasing ultrasonic crushing power (Fig. 2c) and first decreased and then increased with increasing ultrasonic time (Fig. 2d). In this experiment, the minimum particle size of nanobubbles was obtained at 1 s.

The particle size of the nanobubbles in the experiment may have been affected by the ultrasonic energy. In the early stage of ultrasound, liposomes with a large particle size were dispersed by the ultrasound action, so the particle size initially decreased as the ultrasonic time extended. Over time, the ultrasonic energy to the system increased in strength and the particles obtained more energy, allowing them to overcome the repulsive force between each other and cluster, leading to significantly increased size of the detected particles. The later particle size decrease may be related to particle fragmentation and the intermediate state of agglomeration equilibrium, and experimental error is another potential factor. The bubble formation results for the ultrasonic crushing apparatus were also similar, which further supports this inference.

The mass ratio of DOTAP to cholesterol was screened to obtain stable and small liposome nanobubbles. The particle size was smallest when the mass ratio of DOTAP to cholesterol was 1:1 and increased with declining proportion of cholesterol (Fig. 2e). The different proportions of cholesterol on the membrane surface result in liposomes with different properties. Nanobubbles with stable structure do not leak easily and have small particle sizes and concentrated distribution. In this experiment, when the mass ratio of DOTAP to cholesterol was 1:1, the liposomes not only encapsulated the liquid perfluoropentane with fluidity but also guaranteed the stability of the gas core. When the proportion of cholesterol was smaller, stability decreased.

When exploring the influence of perfluoropentane dosage on nanobubble particle size, we found

that particle size gradually increased with higher dosages (Fig. 2f). On the one hand, because the liposomes contain more perfluoropentane, the nanobubble expansion was more obvious. On the other hand, it is possible that the dosage of perfluoropentane was too large to break the nanobubble, or that unfilled perfluoropentane infiltrated the bubbles and interfered with the test.

The pH and concentration of the liposome-forming solvent play an important role in the formation of liposomes and affect their particle size and stability. From the experimental results, it can be seen that the nanobubbles prepared in the glycerol:phosphate-buffered saline (PBS)=1:9 (volume ratio) solution had a larger particle size (Fig. 2g). The motion of the particles is related to the viscosity of the solution. The diameter of nanobubbles prepared in the glycerol: PBS=1: 9 solution was significantly larger because the viscosity of glycerol changed the motion and dispersion characteristics of the particles, making the measured result larger than the real value. Therefore, we used PBS solution as the forming solvent in the experiment.

Lipids generally have their own phase transition temperature points, and detection at different temperatures may affect the state of liposomes, thus affecting particle-size measurement. The particle-size potential analyzer detected different dispersion characteristics and particle sizes for the same nanobubble at different temperatures, and it was found that nanobubble size was larger at 25 °C, and that the particle size of nanobubbles in the same sample decreased significantly at 37 °C (Fig. 2h). This may be closely related to the phase transition temperature of the liposomes. Below the phase transition temperature, the liposomes adhered to each other in the form of colloidal crystals and had poor dispersion. Above the phase transition temperature, liposome fluidity was enhanced, dispersion was uniform, and the detected particle size was reduced.

Based on the results for the above process parameters and preparation methods, we chose the best parameters and process for preparing the liposome nanobubbles. The particle size and potential data are shown in Figs. 3a and S1 and Table S1. The average particle size of the nanobubbles was (224.6±2.4) nm, and the average zeta potential was (46.2±1.3) mV. The electron microscope results (Fig. 3b) also show that the nanobubbles were uniform in size and round in shape.

The DOTAP nanobubbles can be connected with different amounts of CQDs by electrostatic attraction. The zeta potential of the nanobubbles was measured to obtain the extreme value of the coupling of CQDs on the surface of the nanobubble. The results are shown in Fig. 3c. With an increase in the amount of CQDs, the zeta potential changed from positive to negative, and after reaching a certain dose, the zeta potential tended to be stable. The results show that adding 225 μL CQDs (10 mg/mL) into the nanobubble solution can approximate the maximum value of

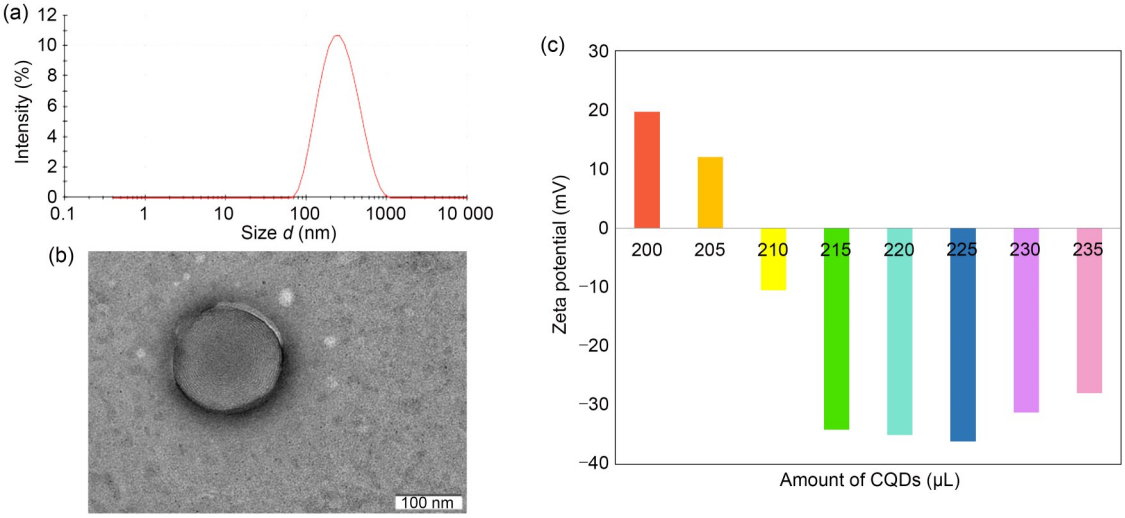

Fig. 3 Characterization of Lip-CQDs. (a) Size distribution of nanobubbles; (b) TEM of nanobubbles; (c) Zeta potential changes after adding different doses of CQDs. CQDs: carbon quantum dots; Lip-CQDs: CQDs-loaded liposome; TEM: transmission electron microscopy.

the nanobubble coupling, and has the highest nanobubble coupling efficiency.

The mice were randomly divided into two groups (Lip-CQDs and Lip) with six mice in each group. Ultrasound images of the tumors were obtained before and after injection of the nanobubbles, and the results are shown in Fig. 4a. Before the solution was injected, the tumor images of the breast cancer model mice were dark because breast cancer is a solid tumor with a faint echo. After 5 min of intravenous injection of nanobubbles, the ultrasound imaging showed significant changes. This indicates that the nanobubbles were able to enter the tumor lacuna and had a strong ultrasonic signal within the tumor. Liposome nanobubbles loaded with CQDs brightened the entire tumor region within 5 min, while nanobubbles without CQDs only gathered in a small area of the tumor. It is possible that the CQDs are negatively charged and can reverse the surface potential of the nanobubble. Nanobubbles with higher negative potentials are more stable and can be better targeted and distributed to tumor sites. The effect of the nanobubbles was also demonstrated in the hepatocellular carcinoma model mice. A cystic tumor was seen in the liver prior to the injection of the nanobubbles but was not easily distinguishable from the surrounding tissue. After the injection of the nanobubbles, we found that the image of the tumor area became clearer.

To observe the real-time distribution of drugs and nanoparticles in major organs, we used an in vivo imaging experiment to analyze the relevant results (Fig. 4b). It was clear that in Hepa1-6 tumor-bearing mice, Lip-CQDs could be enriched in the mouse liver after approximately 5 min and had almost no fluorescence in other organs. Looking at this in combination with the ultrasound imaging results, it was proved that Lip-CQDs can accurately target tumors. The fluorescence in the liver essentially disappeared after 1 h, demonstrating that Lip-CQDs remained in vivo for a short time and could be rapidly metabolized.

The appearance of nanoscale ultrasound contrast agents offers the possibility of ultrasound imaging of extravascular target tissue and promotes more definitive tumor diagnosis. In this study, we prepared liposome nanobubbles with CQDs and tested them for ultrasound imaging. These Lip-CQDs can be used as a new clinical tumor detection preparation because of their contrast-enhancing ultrasound effect and can improve the efficiency and accuracy of clinical tumor detection. In addition, Lip-CQDs can be used for fluorescence detection of tumors. With the continuous crossover and fusion of biomedical and clinical technology, the existing problems of nanoscale ultrasound contrast agents will ultimately be addressed, and the preparation and application prospects for safe and effective nanoscale ultrasound contrast agents will be broadened. We believe that ultrasound contrast agents will play an irreplaceable role in the early diagnosis and accurate treatment of clinical diseases.

Materials and methods

Detailed methods are provided in the electronic supplementary materials of this paper.

Acknowledgments

This work was supported by the National Natural Science Foundation of China (No. 21873057), the Shandong Provincial

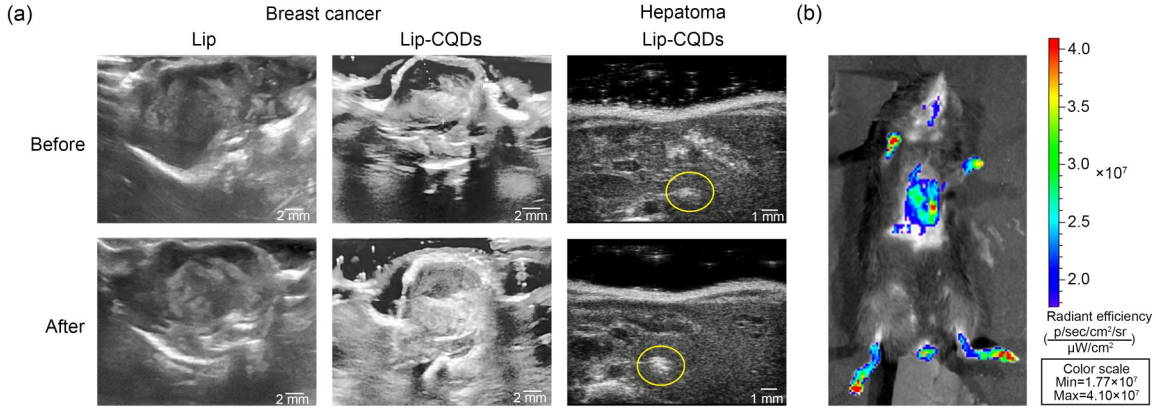

Fig. 4 In vivo imaging of Lip-CQDs. (a) In vivo ultrasound imaging results of Lip and Lip-CQDs; (b) in vivo fluorescence imaging of Lip-CQDs. Lip: liposome; CQDs: carbon quantum dots; Lip-CQDs: CQDs-loaded liposome.

Natural Science Foundation of China (No. ZR2019MB041), and the Fundamental Research Funds of Shandong University (No. 2018JC006), China.

Author contributions

Yankun ZHANG performed the experimental research and data analysis, wrote and edited the manuscript. Yu XIN and Qiong WU performed the establishment of animal models. Lan LIU and Yunxia WANG designed the experiments and wrote this article. Bingtao TANG and Kongxi ZHU gave some good suggestions on the revision of the manuscript, polished English, and checked the final version. Guimei LIN and Hongjuan WANG guided the experiment. All authors have read and approved the final manuscript, and therefore, have full access to all the data in the study and take responsibility for the integrity and security of the data.

Compliance with ethics guidelines

Yankun ZHANG, Bingtao TANG, Yu XIN, Qiong WU, Lan LIU, Yunxia WANG, Kongxi ZHU, Guimei LIN, and Hongjuan WANG declare that they have no conflict of interest.

All institutional and national guidelines for the care and use of laboratory animals were followed.

References

Huang SL, Hamilton AJ, Nagaraj A, et al., 2001. Improving ultrasound reflectivity and stability of echogenic liposomal dispersions for use as targeted ultrasound contrast agents. *J Pharm Sci*, 90(12):1917-1926. https://doi.org/10.1002/jps.1142

Klibanov AL, 2005. Molecular imaging with targeted ultrasound contrast microbubbles. *In*: Bogdanov AA, Licha K (Eds.), Molecular Imaging. Springer, Berlin, p.171-191. https://doi.org/10.1007/3-540-26809-x_10

Paefgen V, Doleschel D, Kiessling F, 2015. Evolution of contrast agents for ultrasound imaging and ultrasound-mediated drug delivery. *Front Pharmacol*, 6:197. https://doi.org/10.3389/fphar.2015.00197

Peng YH, Pei HD, 2021. DNA alkylation lesion repair: outcomes and implications in cancer chemotherapy. *J Zhejiang Univ-Sci B (Biomed & Biotechnol)*, 22(1):47-62. https://doi.org/10.1631/jzus.B2000344

Rathod S, Livergant J, Klein J, et al., 2015. A systematic review of quality of life in head and neck cancer treated with surgery with or without adjuvant treatment. *Oral Oncol*, 51(10):888-900. https://doi.org/10.1016/j.oraloncology.2015.07.002

Willmann JK, Cheng Z, Davis C, et al., 2008. Targeted microbubbles for imaging tumor angiogenesis: assessment of whole-body biodistribution with dynamic micro-PET in mice. *Radiology*, 249(1):212-219. https://doi.org/10.1148/radiol.2491072050

Yang HY, Liu YL, Guo ZY, et al., 2019. Hydrophobic carbon dots with blue dispersed emission and red aggregation-induced emission. *Nat Commun*, 10:1789. https://doi.org/10.1038/s41467-019-09830-6

Zhang Q, Wang RY, Feng BW, et al., 2021. Photoluminescence mechanism of carbon dots: triggering high-color-purity red fluorescence emission through edge amino protonation. *Nat Commun*, 12:6856. https://doi.org/10.1038/s41467-021-27071-4

Zhu SJ, Song YB, Zhao XH, et al., 2015. The photoluminescence mechanism in carbon dots (graphene quantum dots, carbon nanodots, and polymer dots): current state and future perspective. *Nano Res*, 8(2):355-381. https://doi.org/10.1007/s12274-014-0644-3

Supplementary information

Materials and methods; Table S1; Fig. S1